

# PHYSICAL REVIEW D

## PARTICLES AND FIELDS

THIRD SERIES, VOLUME 27, NUMBER 3

1 FEBRUARY 1983

### Semileptonic decays of $B$ mesons

K. Chadwick, J. Chauveau,<sup>(a)</sup> P. Ganci, T. Gentile, Joan A. Guida, R. Kass, A. C. Melissinos,  
S. L. Olsen, R. Poling, C. Rosenfeld, G. Rucinski, and E. H. Thorndike  
*University of Rochester, Rochester, New York 14627*

J. Green, J. J. Mueller,<sup>(b)</sup> F. Sannes, P. Skubic,<sup>(c)</sup> A. Snyder, and R. Stone  
*Rutgers University, New Brunswick, New Jersey 08854*

A. Brody,<sup>(d)</sup> A. Chen, M. Goldberg, N. Horwitz, H. Kooy,<sup>(e)</sup> G. C. Moneti, and P. Pistilli<sup>(f)</sup>  
*Syracuse University, Syracuse, New York 13210*

M. S. Alam, S. E. Csorna, A. Fridman,<sup>(g)</sup> R. Hicks, and R. S. Panvini  
*Vanderbilt University, Nashville, Tennessee 37235*

D. Andrews,<sup>(h)</sup> P. Avery, R. Cabenda,<sup>(i)</sup> D. G. Cassel, J. S. DeWire, R. Ehrlich, T. Ferguson,  
M. G. D. Gilchriese, B. Gittelman, D. L. Hartill, D. Herrup, M. Herzlinger,<sup>(d)</sup> J. Kandaswamy,  
D. L. Kreinick, N. B. Mistry, F. Morrow, E. Nordberg, R. Perchonok, R. Plunkett,  
A. Silverman, P. C. Stein, S. Stone, D. Weber, and R. Wilcke  
*Cornell University, Ithaca, New York 14853*

C. Bebek, J. Haggerty,<sup>(j)</sup> M. Hempstead, J. M. Izen, W. A. Loomis,<sup>(k)</sup> W. W. MacKay,  
F. M. Pipkin, J. Rohlf, W. Tanenbaum,<sup>(l)</sup> and Richard Wilson  
*Harvard University, Cambridge, Massachusetts 02138*

A. J. Sadoff

*Ithaca College, Ithaca, New York 14850*

H. Kagan

*Ohio State University, Columbus, Ohio 43210*

(Received 9 August 1982)

We have studied the production of  $B$  mesons in  $e^+e^-$  annihilations and present new measurements of the semileptonic branching fractions for  $B$ -meson decay. We find  $B(B \rightarrow e\nu X) = 0.127 \pm 0.017 \pm 0.013$  and  $B(B \rightarrow \mu\nu X) = 0.122 \pm 0.017 \pm 0.031$ , where the errors are statistical and systematic, respectively. The observed lepton momentum spectra from  $B$  decays are presented. From these spectra we find the mean hadronic mass ( $M_X$ ) recoiling against the detected lepton to be  $M_X = 2.2 \pm 0.2 \text{ GeV}/c^2$ . We have also observed an enhancement in the lepton yield from the continuum above  $B\bar{B}$  threshold. This enhancement is interpreted as continuum  $B$  production and is consistent with what is expected from the naive quark model.

### I. INTRODUCTION

The discovery of the  $\Upsilon(1S)$  and  $\Upsilon(2S)$  and the evidence for the  $\Upsilon(3S)$  at Fermilab in  $p$ -Be col-

lisions<sup>1</sup> made likely the existence of a new family of  $q\bar{q}$  bound states. Since then, these three states as well as one other, the  $\Upsilon(4S)$ , have been observed in  $e^+e^-$  annihilations.<sup>2</sup> The first three resonances are

all narrow and have been interpreted as bound states of a new-flavored quark and antiquark,  $b\bar{b}$ . The fourth member of this family, the  $\Upsilon(4S)$  at 10.55 GeV, is much broader than the three lighter states, suggesting that it is above threshold for the production of  $b$ -flavored mesons and hence decays rapidly into a  $B$  and a  $\bar{B}$  meson. The  $B$  meson, consisting of the new  $b$  quark bound to a light  $\bar{u}$  or  $\bar{d}$  antiquark, carries the new flavor and therefore must decay through the weak interaction. The observation of enhanced inclusive lepton production in  $\Upsilon(4S)$  decays has been taken as evidence for the weak decay of the  $B$  meson.<sup>3,4</sup>

In this paper we present new results on the decays of  $B$  mesons into states with a single lepton. The data reported here were obtained with the CLEO detector at the Cornell Electron Storage Ring (CESR). The data sample contained 28 000 hadronic events and had an integrated luminosity of 10 600  $\text{nb}^{-1}$ .

## II. THEORETICAL CONSIDERATIONS

The success of the Glashow-Iliopoulos-Maiani<sup>5</sup> mechanism in explaining the interactions of the  $u$ ,  $d$ ,  $s$ , and  $c$  quarks guides us in our expectations for the  $b$  quark. The natural setting to discuss  $b$  decay is the standard model with quark mixing. The standard model of weak interactions uses the  $\text{SU}(2) \times \text{U}(1)$  gauge group of Weinberg and Salam coupled with three left-handed doublets of quarks. The quarks are allowed to mix via the prescription of Kobayashi and Maskawa.<sup>6</sup> In this picture (Fig. 1) the  $b$  mixes with the  $d$  and  $s$  quark, has charge  $-\frac{1}{3}$ , and is grouped with the yet to be discovered  $t$  quark. The absence of flavor-changing neutral currents in this model forbids decays of the  $b$  quark into  $d$  or  $s$  quarks. Since the  $b$  decays via a charged  $W$  and the  $W$  couples to leptons, a prediction of the standard

$$\begin{pmatrix} u \\ d' \end{pmatrix}_L \quad \begin{pmatrix} c \\ s' \end{pmatrix}_L \quad \begin{pmatrix} t \\ b' \end{pmatrix}_L$$

$$\begin{pmatrix} d' \\ s' \\ b' \end{pmatrix} = \begin{pmatrix} V_{ud} & V_{us} & V_{ub} \\ V_{cd} & V_{cs} & V_{cb} \\ V_{td} & V_{ts} & V_{tb} \end{pmatrix} \begin{pmatrix} d \\ s \\ b \end{pmatrix}$$

FIG. 1. Kobayashi-Maskawa model with three left-handed quark doublets. The bare quarks mix according to a matrix which is a function of three angles and a phase parameter. For  $B$ -meson decay the relevant matrix elements are  $V_{ub}$  and  $V_{cb}$ , the coupling of the  $b$  quark to the  $u$  and  $c$  quarks, respectively.

model is that  $B$  mesons should decay to final states with  $e$ 's,  $\mu$ 's, and  $\tau$ 's. The spectator model provides a simple picture for calculating the branching fractions of  $B$  mesons. In this picture (Fig. 2) the light quark does not play a role in the dynamics of the decay. Two predictions of this model are as follows: (1) The semileptonic branching fraction  $B \rightarrow l\nu X$  with  $l=e$  or  $\mu$  should be between 15% and 17% per lepton and (2) on the average there will be approximately one extra kaon in the final state if  $b \rightarrow c$  dominates over  $b \rightarrow u$ . The lower limit on the branching fraction is for the case of  $b \rightarrow u$  only while the upper limit corresponds to all  $b \rightarrow c$ . Taking into account nonspectator effects and hadronic enhancement, Leveille<sup>7</sup> predicts that the semileptonic branching fraction will be 11–13%.

## III. DETECTOR

Figures 3(a) and 3(b) show a front and side view of the CLEO detector. This detector consists of a 1-m-radius solenoidal magnet operating at 4.2 kG. Inside the magnetic field charged particles are detected by cylindrical proportional chambers around the beam pipe and a large cylindrical drift chamber. The rms momentum resolution for particles with momentum greater than 1 GeV/c is approximately  $\delta p = 0.04p^2$  (Ref. 8). Outside the field the detector consists of eight nearly identical octants which provide particle identification. The components of each, moving radially outward from the coil, are a three-layer drift chamber, either a Čerenkov counter or specific ionization ( $dE/dx$ ) chamber, an array of 12 scintillation counters for time-of-flight measurements, and an electromagnetic-shower detector consisting of 44 layers of proportional tube counters interleaved with 1.27-mm-thick lead sheets. An iron absorber ( $\frac{1}{2}$ –1 m in thickness) encloses the detector. A large system of planar drift chambers covering this absorber provides muon identification. Details of the CLEO detector may be found elsewhere.<sup>9</sup>

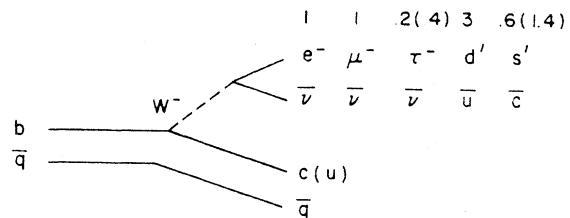


FIG. 2.  $b$ -quark decay in the spectator model. The numbers are phase space times color factors for  $b \rightarrow c$ . The numbers in parentheses are for  $b \rightarrow u$ .

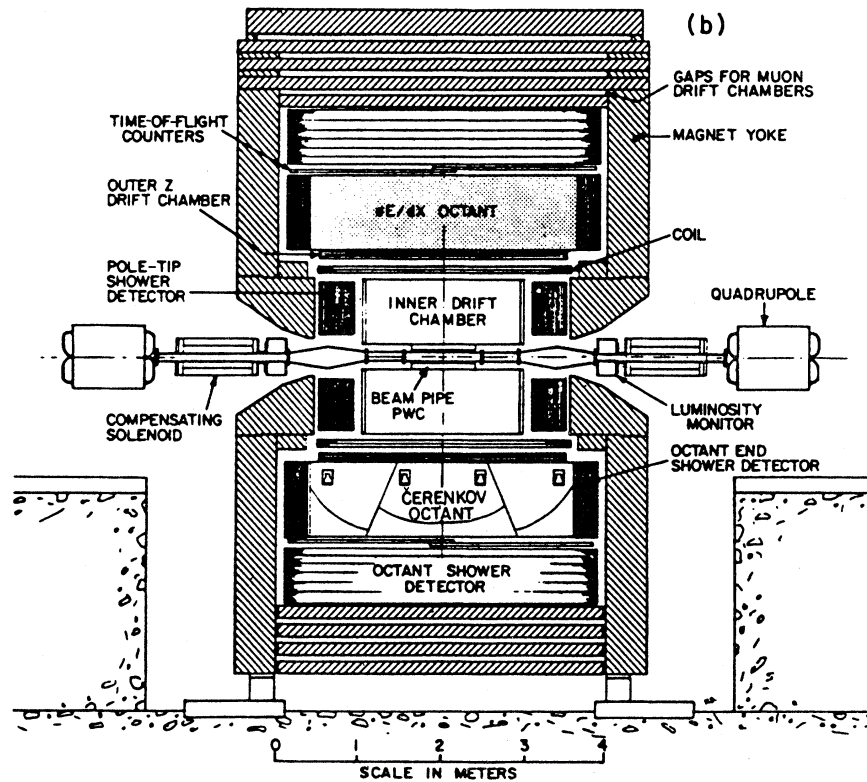
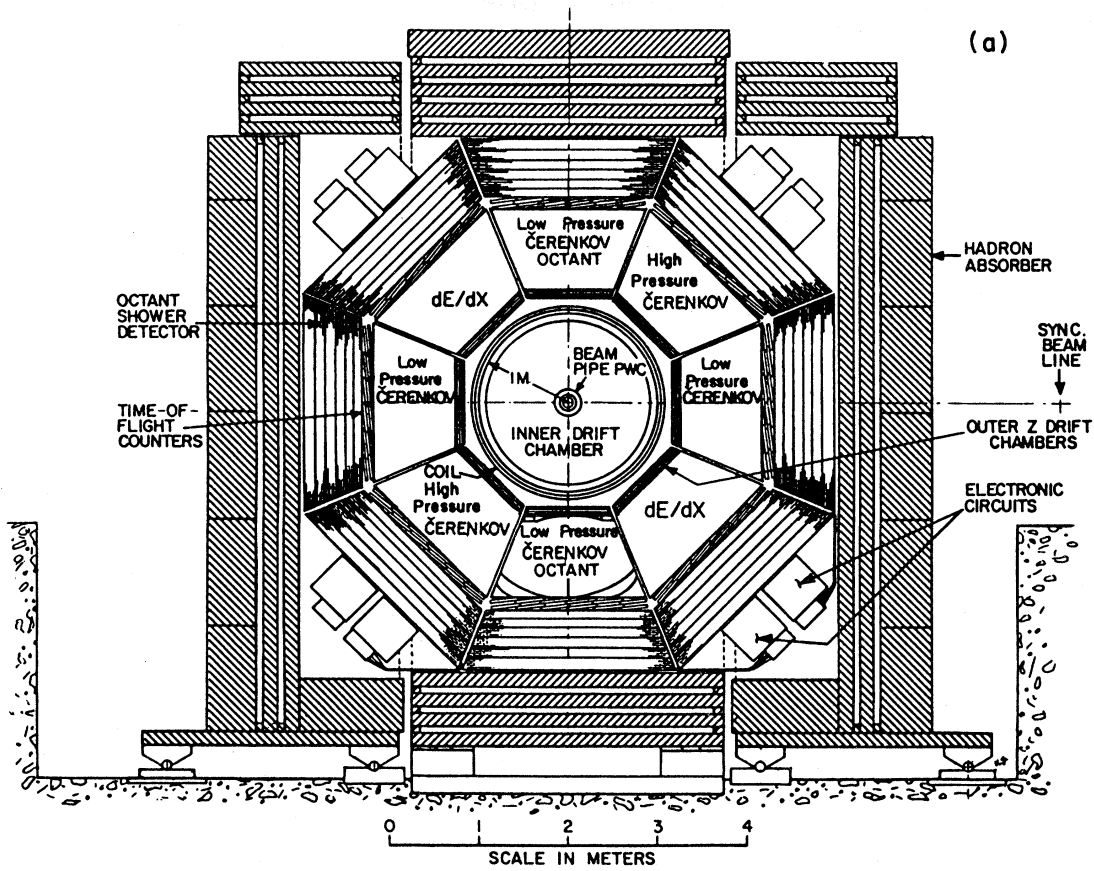


FIG. 3. The CLEO detector: (a) beam's-eye view, and (b) side view.

#### IV. EVENT SELECTION AND DATA ANALYSIS

A total integrated luminosity of  $10\,600\text{ nb}^{-1}$  was collected, of which  $5490\text{ nb}^{-1}$  were on the  $\Upsilon(4S)$  peak,  $3090\text{ nb}^{-1}$  were below the peak,  $1665\text{ nb}^{-1}$  were above the peak, and  $355\text{ nb}^{-1}$  were on the wings of the  $\Upsilon(4S)$ .<sup>10</sup>

Event triggers were examined for hadronic events according to the following rules:

- (1) Each event must have at least five well-reconstructed charged tracks in the drift chamber.
- (2) There must be a common event vertex lying within  $\pm 8\text{ cm}$  of the nominal interaction point along the beam line and within  $\pm 2\text{ cm}$  transverse to the beam.
- (3) At least 250 MeV of electromagnetic energy must be detected in the shower detectors.
- (4) At least 30% of the available energy must be visible as charged tracks in the drift chamber.

The electromagnetic energy cut was chosen to suppress beam-pipe interactions; the charged-energy cut removes two-photon events; and the multiplicity cut eliminates  $\tau^+\tau^-$  events from the data set. These cuts do not significantly degrade the hadronic trigger efficiency. After applying these cuts 19 500 hadronic events were found on the  $\Upsilon(4S)$  peak and 8911 events off the peak. These events were analyzed in order to find high-momentum electron and muon candidates.

The search for electrons was limited to tracks with momenta greater than  $1\text{ GeV}/c$  in order to enhance the signal from  $B$ -meson decay to background processes such as  $\tau$  and  $D$  decay. For the muons there is no fixed momentum cut. The iron absorber imposes a variable momentum cut which depends on the track direction and varies from 1.1 to  $2.0\text{ GeV}/c$ .

A track in a hadronic event with momentum above  $1\text{ GeV}/c$  was an electron candidate if it satisfied the following criteria:

- (1) The track must have had a signal in the electromagnetic-shower detector characteristic of an electron shower: an energy larger than one-half the momentum as measured by the drift chamber, at least 10% of its energy deposited in the first three layers (0.8 radiation lengths) of the shower detector, and an overall average of greater than 1.5 hits per layer.
- (2) It must have had either a Čerenkov signal or a  $dE/dx$  signal with a pulse height consistent with that expected for an electron.
- (3) In selecting electron candidates for the  $B$ -meson branching fraction determination, the track was required to project into a fiducial region of the outer detector where the electron detection had uniform sensitivity.

The electron candidates so selected were then visually scanned by physicists to eliminate four classes of background: Bhabha scattering events with a low-momentum  $\delta$  ray curling up in the drift chamber and thus accounting for several drift-chamber tracks, photons which converted in the beam pipe, photon showers near minimum ionizing tracks, and confusion resulting from many overlapping tracks and a photon in a single octant. The scanning procedure resulted in the elimination of 35% of the electron candidates.

The efficiencies of the electron identification cuts have been studied with a sample of  $\sim 1000$  electrons in the momentum range 1 to  $3\text{ GeV}/c$  derived from radiative Bhabha scattering events, i.e.,  $e^+e^- \rightarrow e^+e^-\gamma$ . The shower-detector cuts described above find  $(90 \pm 1)\%$  of all electrons. The average Čerenkov-counter efficiency was measured to be  $(92 \pm 2)\%$ . The  $dE/dx$  electron identification procedure is based on the following considerations. A  $450\text{-MeV}/c$  pion's signal is 330 and that of a  $3\text{-GeV}/c$  pion is 385. A nonshowing electron will produce a pulse height of 500 units with an rms spread of 30. However, showering in the solenoid coil often causes much larger signals than those stated above. Figures 4(a) and 4(b) show the observed pulse-height spectra from nonshowing particles and electrons. A minimum pulse height cut of 435 was applied to define an electron candidate. The average efficiency of the  $dE/dx$  selection was  $(80 \pm 4)\%$ .

The hadronic background to the electron sample has been estimated by studying pions from reconstructed  $K^0$ 's. Pions fake electrons by undergoing charge-exchange scattering in the coil (8 cm of aluminum) with subsequent photon conversion in one of the electron detectors, or by the overlap between a photon and a charged track. The probability of a pion faking an electron in the shower detector was found to be  $(9.6 \pm 2.5)\%$ . The Čerenkov counter proved very effective in rejecting pions as the threshold for pion detection was  $3.0\text{ GeV}/c$ . Pions of momenta above  $450\text{ MeV}/c$  can produce  $\delta$ -ray electrons which register in the Čerenkov counters, but the cross section for this process is small. The Čerenkov counters have an additional source of background due to particles passing through the phototubes (3% of the sensitive area). The probability of a 1-to- $3\text{ GeV}/c$  pion producing a signal in the Čerenkov counters was measured to be less than 8%. The  $dE/dx$  chambers have sufficient segmentation to help in the recognition of pion tracks that produce large signals due to interactions in the coil. The pion contamination in this system was measured to be  $(16 \pm 5)\%$ .

Charged inner-drift-chamber tracks were con-

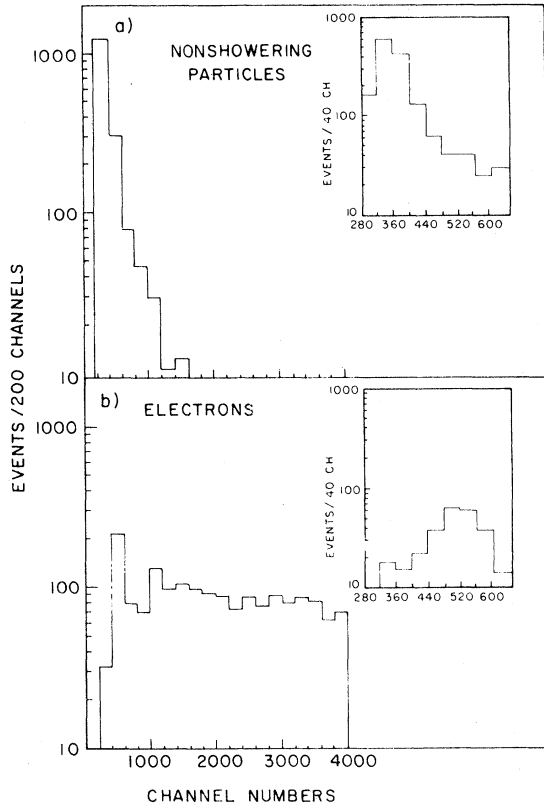


FIG. 4. The observed  $dE/dx$  pulse-height distribution for tracks with  $1.0 < p < 3.0$  GeV/ $c$ . Figure 4(a) contains tracks which do not shower in the proportional tube shower detector. Only  $\Upsilon(3S)$  events with  $R_2 < 0.3$  are used here. Figure 4(b) contains electrons and positrons from radiative Bhabha-scattering events.

sidered muon candidates if they projected in the direction of a muon chamber, had sufficient momentum to penetrate all absorber material along their extrapolated paths, and were matched to two orthogonal muon chambers wires (cross). In this procedure each track was transported through a model of the CLEO detector allowing for ionization losses and multiple scattering in the material. The minimum momentum for penetration ranged from 1.1 to 2.0 GeV/ $c$  with a mean of 1.6 GeV/ $c$ . All events with tracks which satisfied these criteria were visually scanned to eliminate cosmic-ray events. Scanning eliminated approximately 2% of the candidate events.

The efficiency of the muon selection procedure was studied with cosmic rays and  $\mu$  pairs collected during normal data taking. Approximately 90% of the 275 muon chambers were sufficiently well il-

luminated in these events for good efficiency measurements. The average chamber efficiency was 94%. The primary source of inefficiency in muon identification was the process of finding the drift-chamber track and projecting it out to the muon chambers, typically 3–4 m from the interaction point. Figure 5 shows the distribution of the square of the distance between a track projection and an associated muon chamber cross for  $\mu$ -pair events. Those observed with large deviations were generally poorly fitted in the polar angle. The matching cut of 0.32 m was chosen to be considerably larger than the expected contribution of multiple scattering (0.1 m for a 2-GeV/ $c$  track) and track-fitting errors, while still providing good background rejection. On a sample of 671 muon tracks from  $\mu$ -pair events which had crosses in the muon chambers, the matching efficiency was measured to be 82%.

The muon candidate sample included backgrounds from random matches between hadronic tracks and unrelated crosses (noise) in the muon chambers, pion and kaon decay in flight, and hadronic punch through. The random background has been estimated from the data by looking for matches between the tracks of a given event and muon-chamber hits of a previous event. This background varied with time and was measured to be less than 3% of the number of detected muons. The other sources of misidentification cause significant backgrounds in the muon sample. These have been calculated by a procedure described in the next section.

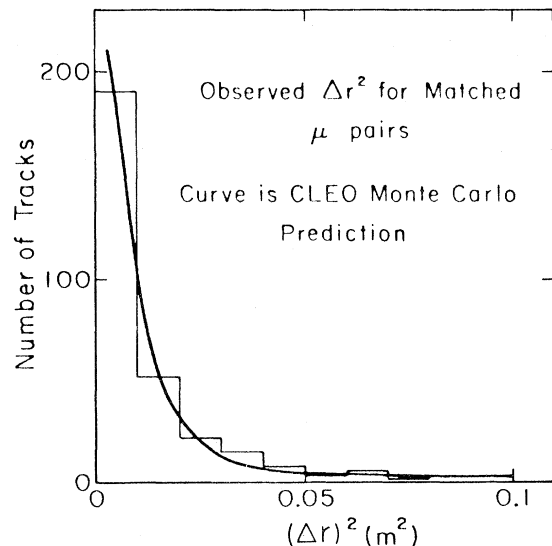


FIG. 5. The observed  $\Delta r^2$  distribution for matched  $\mu$  pairs. The curve is the Monte Carlo prediction for the same distribution.

### V. INCLUSIVE LEPTONS FROM $\Upsilon(4S)$ DECAYS

A total of 522 electrons and 532 muons were found in our sample of hadronic events in the energy range 10.368 to 10.608 GeV. The visible electron and muon cross sections are shown as a function of energy in Fig. 6 and 7, respectively. For comparison Fig. 8 shows the hadronic cross section in the same energy range. A 35% enhancement is observed in the hadronic cross section at the  $\Upsilon(4S)$ , while the lepton cross sections are enhanced by a factor of 2.5. This indicates a large branching fraction into leptons at the  $\Upsilon(4S)$  relative to the continuum. We interpret these leptons as the products of semileptonic decays of  $B$  mesons produced in  $\Upsilon(4S)$  decays. Figures 9 and 10 show the observed momentum spectra for all detected electrons and muons from  $B$  decay. These spectra have been obtained by subtracting the spectra for leptons detected in the continuum below the  $\Upsilon(4S)$  from the spectra for those found on the peak.

Assuming the enhancement in lepton production results from  $B$ -meson decay, we can calculate the semileptonic branching ratio of the  $B$  from

$$B(B \rightarrow l\nu X) = \sigma_l(B\bar{B}) / 2\epsilon_l \sigma_h(B\bar{B}) .$$

In this formula  $\sigma_l(B\bar{B})$  and  $\sigma_h(B\bar{B})$  are, respectively, the enhancement in the inclusive lepton and hadronic event cross sections at the  $\Upsilon(4S)$ , and  $\epsilon_l$  is the detection efficiency for leptons from  $B$  decay. It is assumed that the  $\Upsilon(4S)$  decays 100% into  $B\bar{B}$  where  $B$  is averaged over both the charged and neutral modes, and can be a decay product of a  $B^*$ .

Table I shows the observed yields of electrons and muons in the  $\Upsilon(4S)$  region together with other quantities needed to make background corrections to the lepton signals. The data used in this measurement are independent of the sample used for our

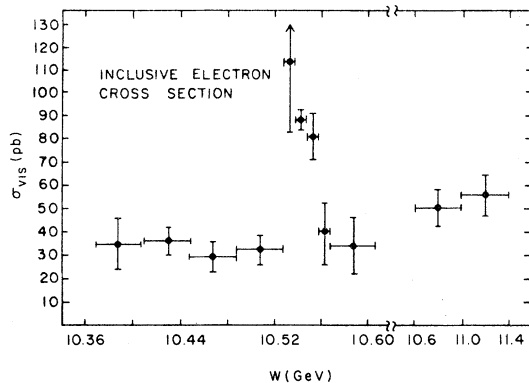


FIG. 6. Inclusive electron cross section as a function of center-of-mass energy.

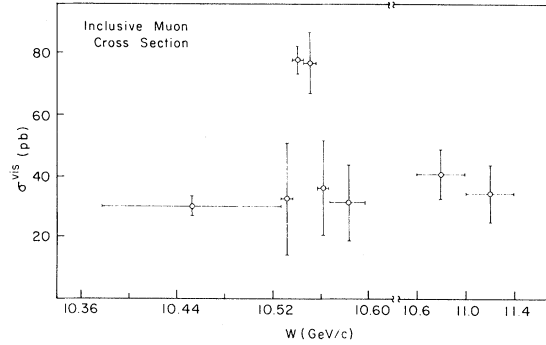


FIG. 7. Inclusive muon cross section as a function of center-of-mass energy.

previous measurements<sup>3</sup> of the  $B$  semileptonic branching fractions.

The lepton-detection efficiency can be written as the product of four efficiencies and acceptances:

$$\epsilon_l = \epsilon_{\text{geo}} \epsilon_p \epsilon_{\text{det}} \epsilon_{\text{anal}} .$$

Each factor will be discussed separately for the electron and muon analyses.

The geometrical acceptances  $\epsilon_{\text{geo}}$  are 0.47 of  $4\pi$  for electrons and 0.78 of  $4\pi$  for muons. The detectable fraction of leptons from  $B$  decay,  $\epsilon_p$ , is defined as the fraction of leptons with measured momenta above 1 GeV/c, and the fraction of muons which penetrate the absorber. These momentum acceptances must be calculated on the basis of some theoretical model. We are guided in the selection of our model by the observed lepton spectra. We have used a phenomenological model of a hadronic system of a fixed mass recoiling against the lepton and neutrino,  $B \rightarrow l\nu X$ . The mass  $M_X$  has been chosen to optimize the fit to the data.

In Fig. 9 we show along with the observed electron spectrum dashed curves which represent the predictions of Monte Carlo calculations for  $B \rightarrow e\nu X$

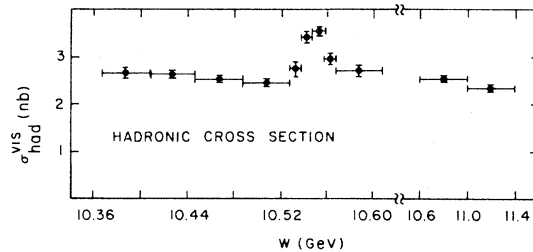


FIG. 8. Inclusive hadron cross section as a function of center-of-mass energy.

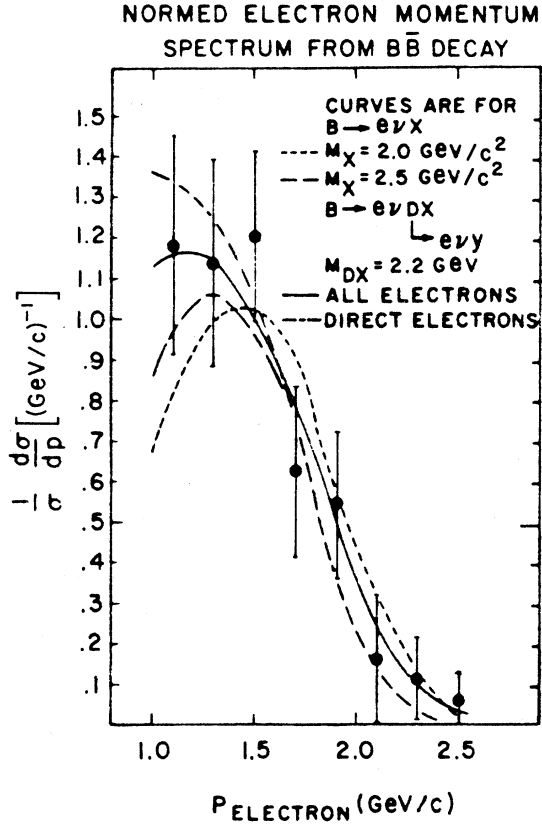


FIG. 9. Electron momentum spectrum from  $B\bar{B}$  events. The curves are Monte Carlo calculations of the electron spectrum for various recoiling hadronic masses. The solid curve includes electrons from  $D$ 's that result from both hadronic and semileptonic  $B$  decay.

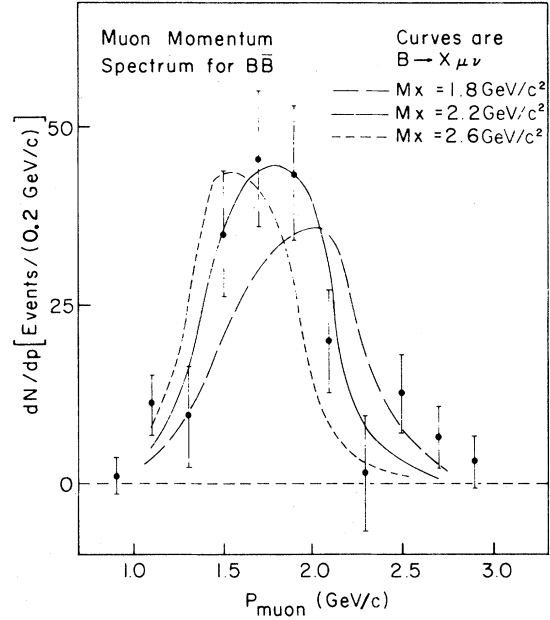


FIG. 10. Muon momentum spectrum from all  $B\bar{B}$  events. The curves are Monte Carlo calculations of the muon spectrum for various recoiling hadronic masses.

via a  $V-A$  current. The mass of the  $B$  meson was taken to be  $5.25 \text{ GeV}/c^2$ . The simulation included radiation in the detector material and the spatial resolution of the drift chamber. Electron tracks in these simulated events were found with our standard

TABLE I. Summary of the numbers used to compute the electron and muon branching fractions of the  $B$  meson.

	On resonance	Off resonance	$B\bar{B}$ decays
Energy (GeV)	10.538–10.558	10.398–10.528	
Luminosity ( $\text{nb}^{-1}$ )	4600	2364	4600
Number of hadronic events	16188	6074	4539 $\pm$ 196
Number of observed electrons	379	77	231 $\pm$ 26
Number of electron-candidate tracks	11972	4769	2825 $\pm$ 1.72
Number of observed muons	351	71	213 $\pm$ 24
Estimated random muons	8	3	
Number of muon-candidate tracks	15697	6525	3183 $\pm$ 199
$\sigma_e$ (pb)	82.4 $\pm$ 4.2	32.6 $\pm$ 3.7	50.2 $\pm$ 5.6
$\sigma_t(\text{electrons})$ (nb)	2.52 $\pm$ 0.03	1.98 $\pm$ 0.03	0.56 $\pm$ 0.04
$\sigma_\mu$ (pb)	74.6 $\pm$ 4.1	28.8 $\pm$ 3.6	46.3 $\pm$ 5.2
$\sigma_t(\text{muons})$ (nb)	3.41 $\pm$ 0.03	2.76 $\pm$ 0.03	0.69 $\pm$ 0.04
$\sigma_h$ (nb)	3.52 $\pm$ 0.03	2.57 $\pm$ 0.03	0.987 $\pm$ 0.043

analysis program. Shown are the curves for  $M_X=2.0$  and  $M_X=2.5$  GeV/ $c^2$ . These bracket the best choice for the recoil mass.<sup>11</sup> The fraction of the generated momentum spectrum greater than 1 GeV/ $c$  for the two cases is 0.83 and 0.71, respectively. The effect of radiation and momentum smearing in track reconstruction is to reduce the number of observed electrons with momentum greater than 1 GeV/ $c$  relative to the number of generated electrons in that range by a factor of 0.87. This factor is relatively insensitive to the decay model. The solid curve is the result of a Monte Carlo calculation for a similar process where the  $X$  particle has been replaced by a  $D$  meson plus one or two pions. The mean mass of the  $D$ -plus-pion system in this case was 2.2 GeV. Included in this calculation are the electrons from  $D$ 's that result from both hadronic and semileptonic  $B$  decay. A model of this type has also been shown to be consistent with measurements for the mean multiplicity of semileptonic  $B$  decays.<sup>12</sup> For this model, 77% of the generated electrons from  $B$  decay have momenta above 1 GeV/ $c$ , while after track fitting 67% of the observed electrons have measured momenta above this value. Thus we have determined  $\epsilon_p=0.67\pm 0.05$  where the error reflects the uncertainty that arises from the range of acceptable fits one can make to the measured spectrum by varying the mean recoil mass from 2.0 to 2.5 GeV/ $c^2$ .

In calculating  $\epsilon_p$  for muon detection we have followed the same procedure but faced the added complication that instead of a sharp momentum cutoff at 1 GeV/ $c$ , we have a cutoff which varies with direction. In Fig. 10 we have plotted the predicted shape of the observed momentum spectrum for  $B\rightarrow\mu\nu X$  with  $M_X=1.8, 2.2,$  and  $2.6$  GeV/ $c^2$ . The  $B$  mass has again been taken as 5.25 GeV/ $c^2$ . The smearing effect of the drift-chamber track-fitting program has been included in this simulation. The result of fits to various  $M_X$  values is that the data favor  $M_X=2.2$  GeV/ $c^2$  ( $\chi^2$  of 9 for 9 degrees of freedom). We take  $M_X=2.2\pm 0.2$  GeV/ $c^2$ . This range of values leads to  $\epsilon_p=0.33\pm 0.08$ .

The detection efficiency  $\epsilon_{\text{det}}$  for electrons is given by

$$\epsilon_{\text{det}} = \epsilon_{\text{sh}}(\epsilon_C + \epsilon_{dE/dx})/2.$$

The efficiency of the electromagnetic-shower detector for identifying electrons,  $\epsilon_{\text{sh}}$ , has been measured to be  $0.90\pm 0.01$ . The average efficiency of the Čerenkov counters and  $dE/dx$  chambers for identifying electrons was  $0.86\pm 0.05$ . Both of these determinations were made with radiative Bhabha events. Combining the two factors, we find  $\epsilon_{\text{det}}=0.77\pm 0.05$ .

For the muon analysis,  $\epsilon_{\text{det}}$  is the efficiency of the

muon chambers. As has been described, individual-chamber efficiencies were measured routinely with cosmic rays and  $\mu$  pairs. An overall muon-detector cross-detection efficiency has been computed by combining the individual chamber efficiencies with weightings determined by the fraction each chamber represents of the total detector acceptance. The overall efficiency was  $0.87\pm 0.05$ . The uncertainty primarily results from the poor illumination of about 10% of the muon chambers by cosmic rays and  $\mu$  pairs.

The analysis efficiency for electrons,  $\epsilon_{\text{anal}}$ , includes the efficiency for finding a drift-chamber track and associating it with a matching shower detector and Čerenkov or  $dE/dx$  signals, and the efficiency of the scanning procedure. Using Bhabha events selected by energy deposited in the shower detector, we found that in 96.5% of the cases studied track reconstruction was adequate to match at least one of the outer detectors. This measurement applies to events with two charged tracks (no more than one per octant). In events of high multiplicity, such as  $B\bar{B}$  events, the matching procedure is more complicated. We have measured the effect of event complexity by studying composite events made by superimposing the raw data hits of electron tracks from radiative Bhabha events on hadronic events. We found our electron-detection efficiency on the embedded event sample was degraded by a factor  $\epsilon_{\text{complex}}=0.79$  relative to that for low-multiplicity events. The scanning efficiency was also determined with the embedded radiative Bhabha events. The composite events were intermixed with, and scanned at the same time as the  $\Upsilon(4S)$  electrons. The scanning efficiency was found to be  $0.92\pm 0.05$ . Comparison of the scanning results of two independent groups of physicists indicated a scanning efficiency of  $0.89\pm 0.02$ , in good agreement. The combined analysis efficiency is  $\epsilon_{\text{anal}}=0.70\pm 0.04$ .

The muon-analysis efficiency measures the ability of the track-fitting program to find and reconstruct a drift-chamber track well enough to match successfully an associated muon-chamber cross. For  $\mu$  pairs this matching efficiency was measured to be 0.82. As in the case of the electrons, this matching procedure is sensitive to event complexity. We studied this effect with composite events created by embedding  $\mu$ -pair hits in hadronic events. In these events our matching efficiency was reduced by a factor of 0.9 compared with the unembedded  $\mu$  pairs. We therefore estimated the analysis efficiency for  $B\bar{B}$  events to be  $\epsilon_{\text{anal}}=0.74\pm 0.05$ .

We can now combine all constituent efficiencies to obtain the overall lepton-detection efficiencies:

$$\epsilon_l = 0.171\pm 0.017 \quad \text{for electrons}$$



and

$$\epsilon_l = 0.167 \pm 0.042 \text{ for muons.}$$

The yields of leptons measured directly for  $B\bar{B}$  include backgrounds which must be estimated and subtracted. The random contamination in the muon signal is subtracted directly from resonance and continuum yields. The enhancements in lepton production from semileptonic  $B$  decay can be expressed as

$$\sigma_l(B\bar{B}) = \sigma_l^{\text{vis}}(B\bar{B}) - \alpha\sigma_t(B\bar{B}) - \beta\sigma_h(B\bar{B}).$$

The subscripts  $l$ ,  $t$ , and  $h$  refer, respectively, to the leptonic cross section, lepton-candidate-track cross section, and the hadronic cross section. These quantities are given in Table I. All cross sections are for  $B\bar{B}$  production and are computed by subtracting the cross sections for the continuum below the  $\Upsilon(4S)$ , extrapolated by  $1/s$  to the  $\Upsilon(4S)$ , from the cross section at the resonance.

The first term  $\alpha\sigma_t(B\bar{B})$  corrects for the misidentification as leptons of particles from  $B$  decay. For the electrons, these are primarily hadronic tracks, but also include photon conversions in the beam pipe. In studying pions from  $K_S^0$  decays, it was found that 3 tracks in 352 were misidentified as electrons yielding a contribution to  $\alpha$  of  $0.0085 \pm 0.005$ . To estimate the contamination from photon conversions, we assume that the production cross section for  $\pi^0$ 's of momentum greater than 1 GeV/ $c$  in the electron fiducial region is one-half that for charged tracks. Only 40% of these contribute, since we only consider electrons of momenta greater than 1 GeV/ $c$ . Each  $\pi^0$  provides two photons, and a photon has a 5% chance of converting in the beam pipe. We assume that we would recognize an electron as coming from a photon conversion if the momentum of the other member of the pair were greater than 25 MeV/ $c$ , so that we would miss approximately 0.025 of the spectrum. The number of electrons which we would not recognize as coming from conversions is then  $0.0005\sigma_t$ . The coefficient  $\alpha$  is the sum of these two terms,  $\alpha = 0.009 \pm 0.005$ .

We have checked this analysis by searching  $\Upsilon(3S)$  data for high-momentum electrons. If one assumes that the narrow  $\Upsilon$  resonances do not decay into final states that pass our hadronic event cuts and include high-momentum electrons, one can use events from these resonances as an electron-free sample to determine the fake probability. In order to reduce the continuum contribution we required, in addition to our usual hadronic-event-defining criteria, that the event have a value of  $H_2/H_0$  less than 0.3.<sup>13</sup> Of 2242 tracks, 22 were called electrons. We calculate that 616 of the tracks and 8.5 of the electrons came from the continuum under the  $\Upsilon(3S)$ , and arrive at

a value  $\alpha = 0.0083 \pm 0.0015$ , in excellent agreement with the value calculated from the  $K_S^0$  pions.

We have estimated the background in the muon signal from hadrons penetrating the iron (punch through) and from decay in flight by studying hadronic tracks in  $\Upsilon(1S)$  events. It was assumed that these data contained no real high-momentum muons. The momentum distribution of hadrons from the  $1S$  is similar to that from the  $4S$ . Our  $\Upsilon(1S)$  sample had 6077 candidate tracks and 39 detected muons with an estimated random contamination of 2. On this basis we calculate  $\alpha = 0.0061 \pm 0.0011$ .

The term  $\beta\sigma_h$  is a correction for the number of leptons in the detected sample which come from the decay of  $D$ 's or  $\tau$ 's produced in  $B$  decay. The contributions of the  $D$ 's and  $\tau$ 's to  $\beta$  are given by the product of the number produced per  $B\bar{B}$  event, the leptonic branching ratio, and the appropriate efficiencies. We assume one  $D$  (or  $D^*$ ) per  $B$  decay. The branching fraction of  $B$  into  $\tau$  has been calculated to be 0.3 times the  $B$  semileptonic branching fractions.<sup>14</sup> With the assumption that we have 50%  $D$ 's and 50%  $D^*$ 's, we obtain an effective semileptonic branching fraction for  $B \rightarrow D$ ,  $D \rightarrow e$  of 9%.<sup>15,16</sup> The branching ratio of  $\tau \rightarrow e$  was taken as 17%.<sup>16</sup> Spectator-model calculations of  $B$  decay predict that 8% of the electrons from  $D$ 's and  $\tau$ 's are above 1 GeV/ $c$ . The efficiency for detecting these electrons is the same as that for primary  $B$ -decay electrons except for the momentum acceptance,  $\epsilon = 0.171 \times (0.08/0.67) = 0.02$ . From this we obtain  $\beta = 0.0032$ .

Making the same assumptions for the muons, and calculating the momentum acceptance for  $\mu$ 's from  $D$ 's to be 0.0086 and that for  $\mu$ 's from  $\tau$ 's to be 0.058, we find  $\beta = 0.0011$ .

With these corrections, we calculate the cross sections for leptons from semileptonic  $B$  decay:

$$\begin{aligned} \sigma_e &= \sigma_e^{\text{vis}}(B\bar{B}) - \alpha\sigma_t(B\bar{B}) - \beta\sigma_h(B\bar{B}) \\ &= 42.0 \pm 5.7 \text{ pb} \end{aligned}$$

and

$$\begin{aligned} \sigma_\mu &= \sigma_\mu^{\text{vis}}(B\bar{B}) - \alpha\sigma_t(B\bar{B}) - \beta\sigma_h(B\bar{B}) \\ &= 41.0 \pm 5.4 \text{ pb} . \end{aligned}$$

The corresponding semileptonic branching ratios are

$$B(B \rightarrow e\nu X) = 0.127 \pm 0.017 \pm 0.013$$

and

$$B(B \rightarrow \mu\nu X) = 0.124 \pm 0.017 \pm 0.031 .$$

The indicated errors are statistical and systematic, respectively. The above systematic errors are highly

correlated and are primarily due to the uncertainty in the Monte Carlo calculations for the lepton momentum spectrum ( $\epsilon_p$ ). The electron and muon branching ratios are in good agreement with each other and also agree well with our previously published measurements.<sup>3</sup> The equality of the electron and muon branching ratios is expected if  $\mu$ - $e$  universality holds in the  $b$  sector.

## VI. INCLUSIVE LEPTONS ABOVE THE $\Upsilon(4S)$

A scan has been made in the energy region above the  $\Upsilon(4S)$  to search for structures of significance comparable to the  $\Upsilon(4S)$ . In the energy range 10.6–11.4 GeV, 1441  $\text{nb}^{-1}$  of data were collected with a total of 3486 hadronic events. No such structures were evident. After making the same cuts as previously discussed for the electron and muon analyses we find 66 electron candidates and 63 apparent muons. A summary of this data appears in Table II, and is plotted in Figs. 6 and 7.

After correcting for contamination in the electron and muon samples we measure the following cross sections:

$$\sigma_e(W \geq 11.0 \text{ GeV}) = 31.0 \pm 5.8 \text{ pb}$$

and

$$\sigma_\mu(W \geq 11.0 \text{ GeV}) = 20.7 \pm 6.1 \text{ pb}.$$

The corresponding corrected cross sections below the  $\Upsilon(4S)$ , scaled to the above- $\Upsilon(4S)$  energy by  $(E_{\text{below}}/E_{\text{above}})^2$ , are

$$\sigma_e(W < 10.54 \text{ GeV}) = 14.5 \pm 3.4 \text{ pb}$$

and

$$\sigma_\mu(W < 10.54 \text{ GeV}) = 10.8 \pm 3.2 \text{ pb}.$$

The step in the total cross section in units of  $\sigma_{\mu\mu}$ , the  $\mu$ -pair cross section,  $\Delta R$ , can be inferred from the step in the lepton cross section,  $\Delta\sigma_l$ , by

$$\Delta R = \frac{\Delta\sigma_l}{2\epsilon B(B \rightarrow l\nu X)} \frac{1}{\sigma_{\mu\mu}}.$$

TABLE II. Summary of electron and muon results in region above the  $\Upsilon(4S)$ .

Energy (GeV)	10.6–11.4
Luminosity ( $\text{nb}^{-1}$ )	1404
Number of hadronic events	3484
Number of observed electrons	66
$\sigma_e$ (pb)	$47.1 \pm 5.8$
Number of observed muons	63
Estimated random events	10
$\sigma_\mu$ (pb)	$37.7 \pm 6.1$

We find  $\Delta R = 0.53 \pm 0.22$  from the electron yield and  $\Delta R = 0.33 \pm 0.23$  from the muon yield. A direct determination of the step in the hadronic cross section measured by CLEO (Ref. 17) has given  $\Delta R = 0.20 \pm 0.08$ , and a similar measurement by the CUSB experiment<sup>18</sup> has yielded  $\Delta R = 0.31 \pm 0.06$ . Simple quark-model considerations lead one to expect a step of  $\frac{1}{3}$  unit of  $R$  for continuum  $B$  production above  $B\bar{B}$  threshold.

## VII. CONCLUSIONS

We have observed large enhancements in the cross sections for electron and muon production at the  $\Upsilon(4S)$  demonstrating the production and decay of  $b$ -flavored hadrons. We have used the spectra of electrons and muons from semileptonic  $B$  decay to determine that the mean effective mass of the hadronic system recoiling against the lepton and neutrino is  $2.2 \pm 0.2 \text{ GeV}/c^2$ . The observed yields of leptons have been used to calculate the semileptonic branching fractions:

$$B(B \rightarrow e\nu X) = 0.127 \pm 0.017 \pm 0.013$$

and

$$B(B \rightarrow \mu\nu X) = 0.124 \pm 0.017 \pm 0.031.$$

These measurements agree well with each other and with our previously reported results. They are lower than what is predicted from a simple spectator model (0.17) but in good agreement with calculations of Leveille that include nonspectator effects (0.11–0.13).

We have measured the electron- and muon-production cross sections in the region above the  $\Upsilon(4S)$  and find them to be consistent with expectations for continuum  $b\bar{b}$  production. The increase in  $R$  above the  $\Upsilon(4S)$  has been measured to be  $0.53 \pm 0.22$  from the electron yield and  $0.33 \pm 0.23$  from the muon yield.

## ACKNOWLEDGMENTS

We are grateful for the efforts of B. D. McDaniel, M. Tigner, R. Littauer, D. Rice, J. Seeman, and the entire CESR operating staff. We acknowledge financial support from the National Science Foundation and U.S. Department of Energy. The work of M. G. D. Gilchriese was supported in part by the Alfred P. Sloan Foundation. The work of R. Wilcke was supported in part by the German Academic Exchange Service.

- (a)Permanent address: LPC, College de France, Paris 75231 Cedex 05, France.
- (b)Present address: LeCroy Research Systems, Spring Valley, NY 10977.
- (c)Present address: University of Oklahoma, Norman, OK 73010.
- (d)Present address: Bell Laboratories, Holmdel, NJ 07733.
- (e)Present address: Xerox Corporation, Rochester, NY 14618.
- (f)Permanent address: University di Roma, I-00185, Rome, Italy.
- (g)Permanent address: Dept. de Physique de Particules Elementaires, Saclay, Gif-sur-Yvette, France.
- (h)Present address: AIRCO Superconductors, Carteret, NJ 07008.
- (i)Present address: Princeton University, Princeton, NJ 08540.
- (j)Present address: Fermilab, Batavia, IL 60510.
- (k)Present address: Schlumberger-Doll Research, Ridgefield, CT 06877.
- (l)Present address: Bell Laboratories, Naperville, IL 60540.
- <sup>1</sup>S. W. Herb *et al.*, Phys. Rev. Lett. **39**, 252 (1977); W. R. Innes *et al.*, *ibid.* **39**, 1240 (1977); K. Ueno *et al.*, *ibid.* **42**, 486 (1979); D. Andrews *et al.*, *ibid.* **45**, 219 (1980); G. Finocchiaro *et al.*, *ibid.* **45**, 222 (1980).
- <sup>2</sup>C. Berger *et al.*, Phys. Lett. **76B**, 243 (1978); C. W. Darden *et al.*, *ibid.* **76B**, 246 (1978); D. Andrews *et al.*, Phys. Rev. Lett. **44**, 1108 (1980); T. Bohringer *et al.*, *ibid.* **44**, 1111 (1980).
- <sup>3</sup>C. Bebek *et al.*, Phys. Rev. Lett. **46**, 84 (1981); K. Chadwick *et al.*, *ibid.* **46**, 88 (1981).
- <sup>4</sup>L. J. Spencer *et al.*, Phys. Rev. Lett. **47**, 771 (1981).
- <sup>5</sup>S. L. Glashow, J. Illiopoulos, and L. Maiani, Phys. Rev. D **2**, 1285 (1970).
- <sup>6</sup>Kobayashi and Maskawa, Prog. Theor. Phys. **49**, 652 (1973).
- <sup>7</sup>J. Leveille, University of Michigan Report No. UMHE 81-18, 1981 (unpublished).
- <sup>8</sup>The momentum resolution of the CLEO detector with a 4.2 kG field is

$$(\delta p/p)^2 = (0.04p)^2 + (0.019/\beta)^2,$$

where  $\beta$  is the particle velocity.

<sup>9</sup>D. Andrews *et al.* (unpublished).

<sup>10</sup>The regions of the  $\Upsilon(4S)$  are defined as follows: below  $\Upsilon(4S)$  is

$$10.398 \leq \sqrt{s} < 10.528 \text{ GeV},$$

wings of  $\Upsilon(4S)$  are

$$10.528 \leq \sqrt{s} < 10.538$$

and

$$10.558 \leq \sqrt{s} < 10.6 \text{ GeV},$$

$\Upsilon(4S)$  is

$$10.538 \leq \sqrt{s} < 10.558 \text{ GeV},$$

and above  $\Upsilon(4S)$  is  $\sqrt{s} \geq 10.6 \text{ GeV}$ . All masses are in CESR energy units.

<sup>11</sup>This result is not very sensitive to the form of the interaction. For instance,  $V-A$ ,  $V+A$ ,  $V$ , and  $A$  all yield acceptable fits to the data with  $M_X$  between 2.0 and 2.5  $\text{GeV}/c^2$ .

<sup>12</sup>M. S. Alam *et al.*, Phys. Rev. Lett. **49**, 357 (1982).

<sup>13</sup>Geoffrey C. Fox and Stephen Wolfram, Phys. Rev. Lett. **41**, 1581 (1978). The variable  $R_2$  is defined as  $R_2 = H_2/H_0$ , where

$$H_l = s^{-1} \sum_{ij} p_i \cdot p_j \cdot p_l (\cos \theta_{ij}).$$

Here  $p_i$  and  $p_j$  are the momenta of particles  $i$  and  $j$ ,  $P_l$  is the  $l$ th Legendre polynomial, and  $\theta_{ij}$  is the angle between particles  $i$  and  $j$ .

<sup>14</sup>N. Cabibbo and L. Maiani, Phys. Lett. **87B**, 366 (1979).

<sup>15</sup>R. Schindler *et al.*, Phys. Rev. D **24**, 78 (1981).

<sup>16</sup>Particle Data Group, Rev. Mod. Phys. **52**, S1 (1980).

<sup>17</sup>CLEO collaboration, contributed paper to the International Conference on High Energy Physics, Bonn, 1981 (unpublished).

<sup>18</sup>E. Rice *et al.*, Phys. Rev. Lett. **48**, 906 (1982).